NISTIR 6030

THIRTEENTH MEETING OF THE UJNR PANEL ON FIRE RESEARCH AND SAFETY, MARCH 13-20, 1996

VOLUME 1

Kellie Ann Beall, Editor

June 1997
Building and Fire Research Laboratory
National Institute of Standards and Technology
Gaithersburg, MD 20899

U.S. Department of Commerce
William M. Daley, *Secretary*
Technology Administration
Gary R. Bachula, *Acting Under Secretary for Technology*
National Institute of Standards and Technology
Robert E. Hebner, *Acting Director*

Characteristics of Oscillating Buoyant Plumes

Baki M. Cetegen and Kent D. Kasper
Mechanical Engineering Department
University of Connecticut, Storrs, CT 06269-3139

Abstract

Experiments on the oscillatory behavior of axisymmetric buoyant plumes of helium and helium-air mixtures are reported for a range of nozzle diameters (3.6 cm. < d < 20 cm.), source velocities and plume densities. Measurements include pulsation frequencies as determined by velocity fluctuations along plume centerline and phase resolved laser Doppler velocity measurements. These non-reacting buoyant plumes are found to exhibit periodic oscillations of plume boundaries as well as formation of toroidal vortices within one-half diameter above nozzle exit. These oscillations and vortices are similar to those observed in pool fires, although their frequency scaling is somewhat different. The frequency relationship is well represented by the expression $S = 0.83\ Ri_1^{0.38}$ where $S = fd/V$ and $Ri_1=[(\rho_\infty - \rho_p)\ g\ d] / \rho_\infty\ V^2$. Here, f, V, ρ are frequency, source velocity and density and subscripts f and ∞ refer to plume fluid and ambient respectively. Around $Ri_1 = 100 - 500$, there is a transition in the frequency scaling as evidenced by more turbulent and vigorously mixing plumes beyond the transition. Above this transition, S scales with $Ri_1^{0.28}$. Phase resolved velocity field of a pulsating buoyant plume reveals a strong buoyant acceleration along the plume centerline followed by a deceleration in the region of toroidal vortex formation. The strong upward acceleration is also accompanied by a radial inflow which determines the entrainment characteristics of these pulsating buoyant plumes.

INTRODUCTION

Periodic pulsations have been observed in pool fires by many investigators including the research group of Prof. Zukoski at Caltech. Oscillations of plume boundaries near the origin of a pool fire result in the formation of toroidal vortical structures which rise through the visible flame region and influence its characteristics such as entrainment, flame height and radiation. Although effects of these pulsations on flame properties have been contemplated by some researchers, it has been put into quantitative use for the first time by Zukoski et al [1] in explaining fluctuations observed in visible flame heights. It is generally believed that inclusion of the effects of these oscillations (frequency and strength of generated vorticity) will result in better description of entrainment process in pool fires and enable better scaling relationships. The first author had the privilege to be part of the fire research group of Prof. Zukoski in the early eighties. Motivation for this work has originated from fire research at Caltech during this time. It is therefore fitting to present some of our recent results on buoyancy induced instabilities in non-reacting buoyant plumes.

Strongly buoyant non-reacting plumes, although somewhat different than pool fires, have been observed to exhibit oscillatory behavior similar in appearance to pool fires. In fact, our earlier experiments with Helium plumes and simulated pool fires [2] have suggested that oscillations are initiated solely as a result of high buoyancy near the source of a plume. In our study , we have examined only a limited number of helium plumes and compared their behavior to pool fires and concluded that oscillation frequency scaling was similar to pool fires. However, Hamins et al [3] reported that non-reacting buoyant plumes of helium had a somewhat different frequency scaling than that for pool fires. In contrast to well accepted scaling of pool fire pulsations with the inverse square root of source diameter, $D^{-0.5}$, non-

reacting buoyant plumes appear to exhibit different scaling as $D^{-0.62}$. Recently, Delichatsios [4] conducted a dimensional analysis of pulsation frequency and showed that buoyant plume frequency should scale as $D^{-2/3}$. In order to further investigate the mechanism responsible for these pulsations, we embarked on an experimental investigation with two main objectives. First objective was to determine the pulsation frequency scaling for non-reacting buoyant plumes for a wide range of source parameters (source diameter, velocity and fluid density), conveniently grouped as a Froude or Richardson number. Second objective was to characterize the flow field in the region of vortex formation to examine its key features during the formation and advection stages of toroidal vortices to help understand the mechanism of this instability.

EXPERIMENTAL

The experimental set-up was designed to conduct detailed velocity measurements by conditional laser Doppler velocimetry as well as to determine the pulsation frequencies of buoyant plumes originating from circular nozzles of 3.6, 5.2, 7.3, 10.0, 15.2 and 20 cm. diameter. Nozzles were constructed from either PVC or metal pipe with tapered outside surfaces at 10° with a lip thickness of 1 mm at the exit. The length to diameter ratio ranged from 3 to 10 for all nozzles with the large values for smaller diameter nozzles. A 64 mesh, flat stainless steel screen was placed across the nozzle exit. The main purpose of this screen was to provide a uniform flow condition at the nozzle exit which was otherwise impossible due to rapid buoyant acceleration of helium with respect to the surrounding air medium. Presence of screen prevented backflow of air upstream of nozzle exit and also insured a plug flow exit condition. In large nozzles, with $L/d \approx 3 - 4$, a honeycomb flow straightener was also placed for flow uniformity upstream of nozzle exit. These nozzles were placed vertically in draft free surroundings as shown in Figure 1. Twenty mesh window screens were formed into a circular cylinder far from the nozzles (D = 2 m) to ensure little or no influence of turbulent eddies that might be present in room air. Studied plumes were free of any forced draft above so that no artificial downstream influence was imposed.

Characterization of plume oscillation frequencies was facilitated by a total pressure probe placed along the plume centerline at a height of 0.5 d. Selection of this location was such that large velocity oscillations in vortex formation and convection phases can be easily detected by the pressure probe. The pressure port was connected by a short Tygon tubing to the high pressure side of a differential pressure transducer of capacitance type (Setra Model 264 +/- 0.05 inch of H_2O column) while the low pressure side was exposed to ambient pressure. Considering the total pressure $P(t) = P_o + \rho U^2(t)/2$, where P_o is the static pressure, ρ is density and U(t) is the time varying velocity at the probe tip, the differential pressure transducer responds to variations in the square of velocity. The pressure transducer output was first amplified (Tektronix AM502) and filtered by a low pass filter before being processed by a frequency spectrum analyzer (Analogic Data 6000). An example of the pressure trace and its fast fourier transform (FFT) is shown in Figure 2 for a helium plume originating from the 10 cm. diameter nozzle. The frequency peak at 4.5 Hz is unambiguously associated with the pulsation frequency of this helium plume. The frequency peaks below and above this fundamental frequency represent subharmonics and superharmonics of 4.5 Hz. Figure 3 shows a sequence of photographs of this plume as obtained by laser Mie scattering from small water droplets. These photographs, obtained at 15 fps, also suggest that a complete pulsation cycle (for example, frames 1 to 7) occurs at around 5.0 Hz. The probe acoustic response to pressure oscillations was determined based on an analysis by Greitzer and Nikkanen [5] with an estimate of 13 milliseconds for the probe/sensor configuration in our experiments. This value is considerably smaller than the typical period of studied plume oscillations in the range 0.07 to 0.5 seconds.

The velocity field of an oscillating buoyant plume of helium-air mixture was mapped using conditional Laser Doppler Velocimetry using the 10 cm. diameter nozzle. The nozzle was

surrounded by a co-flow chamber, as shown in Figure 1, which provided the external particle seeding in the rapidly contracting region of the plume near the nozzle exit. The plume was seeded with water droplets from two different seeders. Seeding of the core helium air flow was accomplished by a six jet droplet generator (TSI Model No. 9306) while the co-flow seeding was affected by a domestic ultrasonic humidifier. Droplets from both seeders were measured to be less than 2 μm by a phase Doppler particle sizer. The LDV system was a conventional single component velocimeter operating in the backward scatter mode.

Data collection from the pressure transducer and the LDV system was handled by an IBM PC/XT computer, interfaced with two Data Translation DT2801 A/D acquisition boards, running a FORTRAN controlling program. Two methods can be employed to carry out conditional data acquisition. One method is continuous acquisition of the "control" and the measured signals and post processing those data to obtain conditionally averaged quantities. Another method is to trigger the data acquisition only when the condition on the control signal is satisfied. The first method requires high data rates in order to reconstruct conditionally averaged velocities at all phases. However, the second method becomes desirable in situations where the data rate is dependent on uncontrollable factors such as local particle seeding density in the flow. Data were collected by this second method by triggering velocity data acquisition at four phases along the sinusoidal pressure signal: the maximum point (phase A), the negative slope zero crossing (B), the minimum point (C) and the positive slope zero crossing (D). At each spatial location, data acquisition continued until 100 data points were collected at each phase. Experimental uncertainty in the velocity measurement was less than 3 % in the central part of the plume and up to 13 % near the plume edges. Further details of data acquisition procedures can be found in reference [6].

RESULTS AND DISCUSSION

Frequency Measurements

As described in the previous section, a number of experiments were conducted to determine the relationship of plume oscillation frequency to plume parameters. The first set of experiments dealt with pure helium plumes emanating from nozzles of diameters: 3.6, 5.2, 7.3, 10.0, 15.2, and 20.0 cm. In a second set of experiments, mixtures of helium and air were injected through the same nozzles to determine effects of plume density on oscillatory behavior. Parameters in this problem are nozzle exit velocity, V, nozzle diameter, d, gravitational acceleration, g, plume density, ρ_p, and the atmospheric density, ρ_∞. In the case of pool fires and turbulent reacting jets, variable density effects arise due to the chemical composition and temperature changes which result from exothermic combustion reactions. In the absence of combustion, variable densities arise from compositional variations due to mixing of different density fluids. The aforementioned quantities can be formed into a number of non-dimensional groups given by:

Strouhal number	$S = fD / V$ where $V = V_o$ or $\sqrt{gd}$ or $\sqrt{\Delta\rho gd/\rho}$
Density parameter	$\Pi_1 = (\rho_\infty - \rho_p)/\rho_\infty$ or $\Pi_2 = (\rho_\infty - \rho_p)/\rho_p$
Richardson number	$Ri_o = g\,d / V_o^2$ or $Ri_1 = \Pi_1\, Ri_o$ or $Ri_2 = \Pi_2\, Ri_o$
Froude number	$Fr_j = Ri_j^{-1}$

Strouhal number describes a non-dimensional oscillation frequency. Density ratio can be constructed with either the ambient fluid or the plume density in the denominator as indicated by Π_1 or Π_2. Richardson (or inverse Froude) number is a measure of the ratio of buoyancy force to jet momentum. Combinations of these parameters, also being dimensionless, may also be constructed. While the primary dimensionless parameters have been listed in terms of nozzle exit velocity, it can be envisioned that a more relevant velocity scale in buoyant flows can be taken as $\sqrt{gd}$, or more appropriately as $\sqrt{\Pi_1 gd}$ or $\sqrt{\Pi_2 gd}$.

Experiments were conducted with variations in source diameter, nozzle exit velocity and plume density at the source such that a universal correlation of the form $S= f(Ri_j,\Pi_j)$ can be established. The plume gas density at the source was varied by mixing helium with air at different proportions. When plotted in the form of $S = f(Ri_o)$, data for helium-air mixture plumes exhibited significant deviations from pure helium data. These non-dimensional parameters, also used by Hamins et al [3] to correlate flame and non-reacting plume pulsation frequencies, do not account for the density difference between the plume fluid and its surroundings which, in buoyant flows, provides the driving force for the buoyant fluid motion. While these non-dimensional parameters produce reasonably good correlations of flame and helium plume data because of their similar densities, they do not take account of differing plume fluid densities in general. The density effect was then introduced in Richardson number as $Ri_1 = \Pi_1 Ri_o$ or $Ri_2 = \Pi_2 Ri_o$. Initially, data were plotted using both parameters. It was found however that Ri_2 yielded a much poorer correlation of data than Ri_1 even though Ri_2 is the more appropriate form of Richardson number. Figure 4 shows the correlation of data in the form of $S = f(Ri_1)$. These parameters correlate data for all plumes well, leading to the expression $S = 0.83\ Ri_1^{0.38}$ for $Ri_1 < 100$ This correlation also agrees well with that developed by Hamins et al [3]. While this correlation is satisfactory for the majority of the data, helium plume data for 15 and 20 cm. nozzle diameters do not follow this correlation beyond $Ri_1 = 100$. In the region $Ri_1 > 100$, frequency data appear more scattered and exhibit a different scaling as $S \alpha Ri_1^{0.28}$. A closer examination of the experimental data for d = 15 and 20 cm. diameter nozzles indicate that changes occur in plume structure between $Ri_1 = 100$ and 500. This transitional behavior had not been observed in other studies as far as we know.

In order to determine the origin of this transition, visual observations and frequency spectra of two pure helium plumes originating from 10 cm. and 20 cm. diameter sources lying below and above the transition were compared. In figure 6a, a photograph and pressure-time trace for a helium plume originating from the 10 cm. diameter source are shown for $Ri_1 = 220$, $Re_d = 50$. The plume starts with a laminar flow field as it rapidly contracts due to buoyancy. There appears to reside an air bubble in the center of the plume penetrating all the way close to the nozzle surface. The upper portions of the plume exhibit transition from laminar to turbulent in the region where a toroidal vortex is formed. For this plume, pressure (or velocity) oscillations are periodic with an apparent long period modulation of its amplitude as seen in Figure 2a. The resulting frequency spectrum shows a single distinct peak associated with the visual pulsations as shown in Figure 7a. In contrast, a helium plume emanating from the 20 cm. diameter nozzle with $Ri_1 = 470$ and $Re_d = 96$ exhibits a significantly more turbulent appearance as shown in Figure 6b. This plume, typical of all plumes above the transition, is more turbulent at its source with considerable amount of air penetrating to its base. The velocity fluctuations are of a less periodic and more chaotic nature compared with the previous case, representative of plumes below transition. In fact, the frequency spectrum, in Figure 7b, contains a number of dispersed peaks around the highest peak associated with puffing. This difference is believed to be the major reason for the change in the frequency scaling.

Pulsation frequencies were non-dimensionalized using the nozzle exit velocity in the correlations presented above and by Hamins et al [3]. Although the source velocity plays a role very close to the nozzle exit, it is expected that the buoyant acceleration rapidly takes over and a buoyant velocity scale may be more appropriate. In figure 5, Strouhal numbers based on two different velocity scales are shown as a function of Ri_1. Figure 8a shows the Strouhal number based on the buoyant velocity scale of $\sqrt{gd}$. It appears that this scaling results in poorer correlation of data for individual data sets as well as the large amount of scatter for some data. It, however, is not the proper velocity scale since it does not contain a density difference which drives the buoyant motion. Thus, a modified velocity scale of $\sqrt{(\rho_\infty - \rho_f)gd/\rho_\infty}$ was introduced in Figure 5b. This velocity scale produces a significantly better correlation of data similar to that

of Figure 4. The resulting correlation can be expressed as $S_2 = 0.83\ Ri_1^{-0.12}$ for $Ri_1 < 500$. This correlation can be shown to be identical to that obtained from Figure 4.

Scaling differences between pool fires and non-reacting buoyant plumes arise due to change in buoyancy flux with downstream distance. In pool fires, the total buoyancy flux increases with downstream distance due to local heat release yielding $f \alpha d^{-1/2}$. In non-reacting buoyant plumes, total buoyancy flux is constant and buoyancy is reduced locally by mixing above the plume source resulting in $f \alpha d^{-0.62}$. An explanation of this scaling has been recently given by Delichatsios [4]. It should be noted however that there exists an overlap region where pool fire and non-reacting buoyant plume oscillations exhibit similar values of Strouhal numbers. Our earlier data [1] from a 10 cm. diameter source were obtained in this overlap region. It was then conjectured that flames and helium plumes exhibited similar pulsation frequency characteristics.

Plume Velocity Field:

Phase-resolved velocity measurements were performed on a helium-air mixture plume originating from a 10 cm. diameter nozzle using laser Doppler velocimetry. Plume parameters were $Ri_1 = 50$, $Ri_2 = 195$, plume density ratio, $\rho_p/\rho_\infty = 0.26$. The co-flow velocity was set at 2.4 cm/s, providing minimal interference to plume development. Measurements were concentrated in a region spanning one nozzle diameter height from the nozzle centerline to the nozzle edge. Radial extent of these measurements was limited by available seeding. Although a co-flow chamber provided external seeding at low velocity outside the plume boundary, this stream was quickly ingested into the plume near the vortex formation region. Figure 8 shows the velocity measurements at four instants during one pulsation period. Phase A corresponds to the maximum in the pressure signal, followed by Phase B at the negative slope zero crossing, Phase C at the minimum and Phase D at the positive slope zero crossing. At all phases of plume motion, a strong buoyant acceleration along the plume centerline is evident. Centerline velocity increases from few tens of centimeters per second to over one meter per second in a distance of several centimeters.

At phase A, representing the instant at which plume centerline velocity at $z = d/2$ is maximum, strong axial acceleration occurs over the central 10 - 15 mm. radial region. This is where a toroidal vortex ring is formed. In fact, the toroidal vortex is formed at a height around $z \approx d/2$ as it can be seen in Figure 3. The axial acceleration is also accompanied by a strong radial inflow towards the plume axis near the base. At phase B, toroidal vortex has convected downstream and continues its influence by its induced higher flow velocities behind it. The radial velocity components are somewhat lower than those at phase A, where vortex is closer to the nozzle. At phase C, the toroidal vortex has completely moved out of the measurement region. However, a strong centerline acceleration is still maintained at this instant with lower velocity magnitudes for $z \leq d/2$. Finally, at phase D, the velocity field becomes more uniform and vertically oriented as the strong flow acceleration is re-established between phases D and A.

In addition to the vector plots delineating the general features of the velocity field, the vertical velocity components are plotted in Figure 9. Velocity profiles near the nozzle exit are approximately of "top-hat" shape with rapid acceleration ensuing a short distance above. In particular, velocity profiles deviate considerably from the conventional Gaussian profiles in the region of the toroidal vortex. The maximum velocities occur off-axis and the profiles exhibit inflection points at 50, 60 and 70 mm. locations at phase A. In this vortex formation region, superposition of viscous vortex velocity profile on its convection speed yields these off-center peak velocity distributions. Downstream convection of the vortex can be followed in this figure as indicated by the arrows shown.

In understanding plume oscillation mechanism and the underlying flow dynamics, characteristics of buoyant acceleration along the plume centerline can supply valuable

information. Figure 10 shows plume centerline velocity distributions at four instants during the pulsation cycle. The most striking feature is the rapid acceleration at phase A, followed by a deceleration with the peak velocities occurring around $z \approx 60$ mm. It is precisely in this region where the toroidal vortex formation is initiated by transfer of axial momentum to radial motion. At later phases (B & C), flow velocities are lower below this location due to stagnation behind the vortex and higher above because of the induced suction behind the convecting toroidal vortex. These results imply, as suggested earlier [2], that toroidal vortex formation is a result of rapid buoyant acceleration of light plume fluid in heavier, more or less quiescent surroundings. Once this toroidal vortex forms, it affects the surrounding flow field as it convects upward. Then, its influence decays near the plume source, setting up a strong acceleration in the lower region of a buoyant, non-reacting plume for the next cycle.

CONCLUSIONS

It has been found experimentally that non-reacting buoyant plumes undergo quasi periodic oscillations of the type observed in pool fires. Although the characteristics of the plume instability appear to be similar in both cases, the frequency scaling with source diameter is somewhat different yielding $f \alpha d^{-0.62}$ for non-reacting plumes versus $f \alpha d^{-1/2}$ for pool fires. In earlier correlations of pulsation frequency of the form $fd/V = f(gd/V^2)$, the density difference between the plume fluid and the surrounding medium was omitted. Our experimental data for plumes of helium-air mixtures correlate significantly better with respect to Richardson number defined as $[(\rho_\infty - \rho_p)\, g\, d]/\rho_\infty V^2$. In fact, the velocity scale used in forming the Strouhal number can also be taken as a buoyant velocity scale $\sqrt{(\rho_\infty - \rho_p)gd/\rho_\infty}$. There exists a transition in the scaling of pulsation frequency around $Ri_1 = 100$ -500. This transition is associated with the rapid turbulent mixing of the plume fluid with its surroundings close to the nozzle exit. To our best knowledge, this transition has not been reported before.

Phase resolved velocity measurements in a periodic helium plume clearly show the various stages during one oscillation cycle. A rapid buoyant acceleration of plume fluid near the centerline is followed by the formation of a toroidal vortex ring around a height of one-half of the source diameter. As this vortex ring convects downstream, it retains its influence on the upstream flow field. Finally, buoyant acceleration reestablishes the formation of the next toroidal vortex. Velocity profiles within the plume are influenced by the presence of the toroidal vortex. Velocity profiles exhibit peak velocities that are displaced from the plume centerline in the region of the toroidal vortex.

REFERENCES

1. Zukoski, E. E., Cetegen, B. M. and Kubota, T., Twentieth Symposium (International) on Combustion, The Combustion Institute, Pittsburgh, p.361. 1984
2. Cetegen, B. M. and Ahmed, T. A., Experiments on the Periodic Instability of Buoyant Plumes and Pool Fires, Combustion and Flame, 93:157-184. 1993
3. Hamins, A., Yang, J. C., and Kashiwagi, T., Twenty-Fourth Symposium (International) on Combustion, The Combustion Institute, Pittsburgh, p.1695. 1992
4. Delichatsios, M. A., "Gravitational Fluctuations in Pool Fires and Pool Buoyant Flows", to appear as a technical note in Combustion Science and Technology
5. Greitzer, E. M. and Nikkanen, J. P., Pratt & Whitney Aircraft Inter-Office Correspondence, December 17, 1971.
6. Kasper, K. D., An Experimental Investigation of Naturally Oscillating Buoyant Plumes of Helium/Air Mixtures, M.Sc. Thesis, University of Connecticut, (1995)

Acknowledgments

The research reported herein had been supported by National Science Foundation Grant (CTS-8909176). Additional support from UConn. Research Foundation is acknowledged.

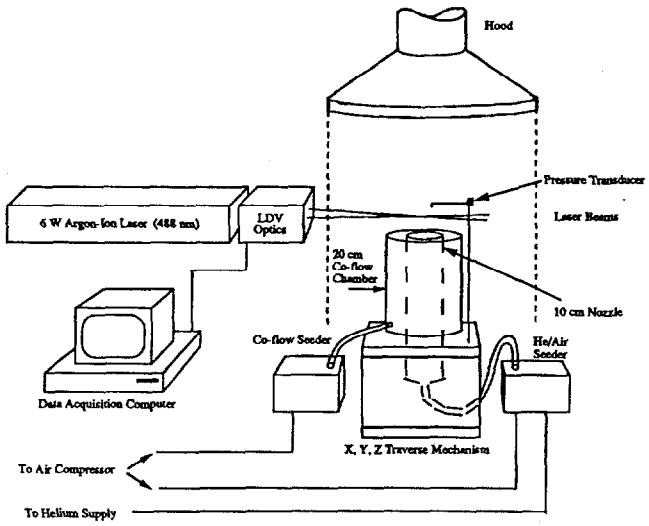

Figure 1. Schematics of the experimental set-up

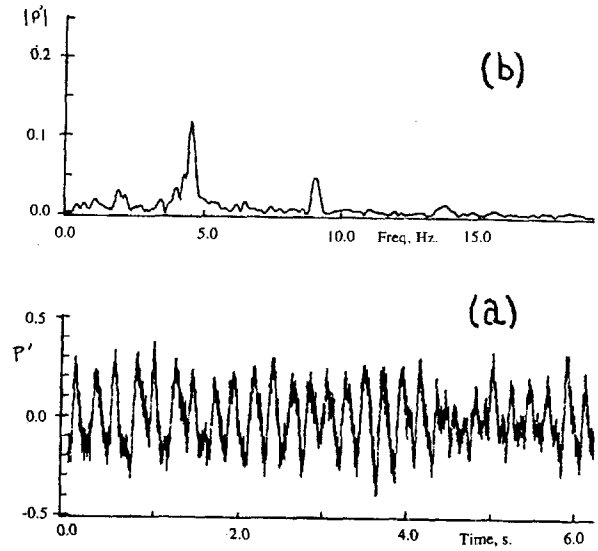

Figure 2. Plume centerline pressure fluctuations (a) and its frequency spectrum (b) for a helium plume originating from a 10 cm. diameter nozzle at $Ri_l = 316$.

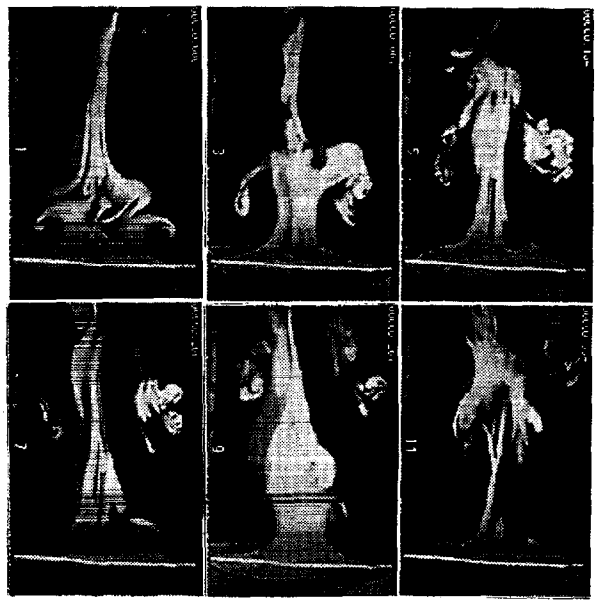

Figure 3. Sequence of images of a helium plume originating from a 10 cm. diameter source with $Ri_l = 316$. Framing rate is 15 fps.

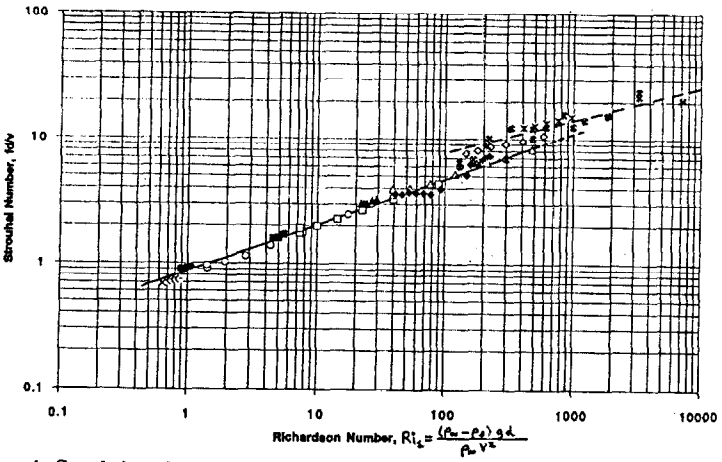

Figure 4. Correlation of pulsation frequency in terms of Strouhal number and Richardson number, Ri_d. Helium plumes: + d = 3.6 cm, o d = 5.2 cm., □ d= 7.3 cm., Δ d = 10.2 cm., ◇ d = 15.2 cm., ⊕ d= 20.3 cm. Helium -air mixtures: × d = 3.6 cm, • d = 5.2 cm., ■ d= 7.3 cm., ▲ d = 10.2 cm., ◆ d = 15.2 cm., ✳ d= 20.3 cm.

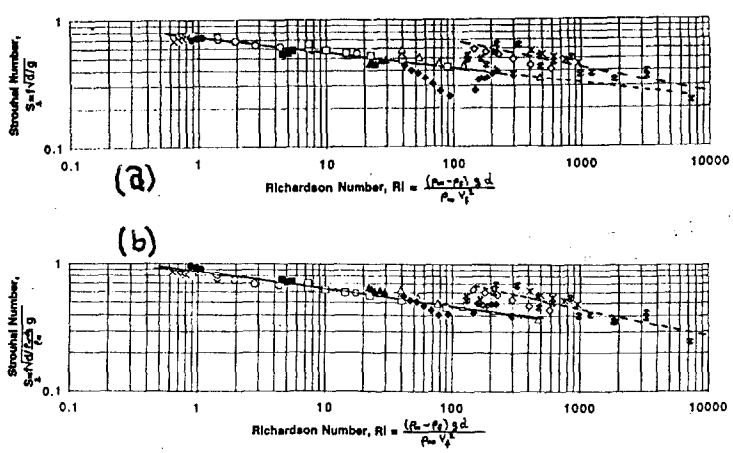

Figure 5. Correlation of pulsation frequency in terms of different definitions of Strouhal numbers (a) $S = f\sqrt{d/g}$, (b) $S = f\sqrt{d/(1-\rho_f/\rho_\infty)g}$ as a function of Ri_l

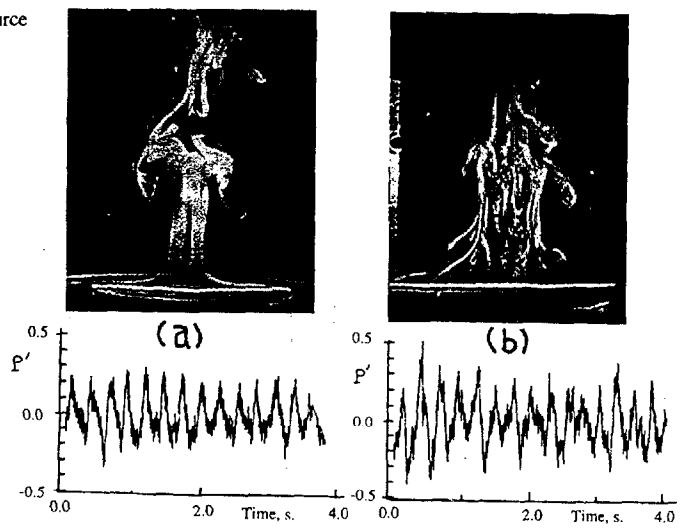

Figure 6. Plume images, pressure-time trace for helium plumes originating from (a) d=10 cm. at $Ri_l = 220$, $Re_d = 50$ (b) d= 20 cm. at $Ri_l = 470$, $Re_d = 96$.

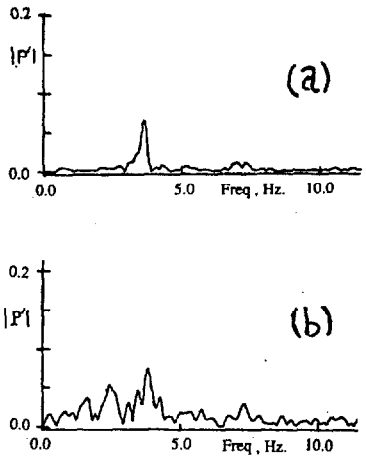

Figure 7 (top) Pulsation frequency spectra for the plumes of figure 6 (a) d = 10 cm. (b) d = 20 cm.

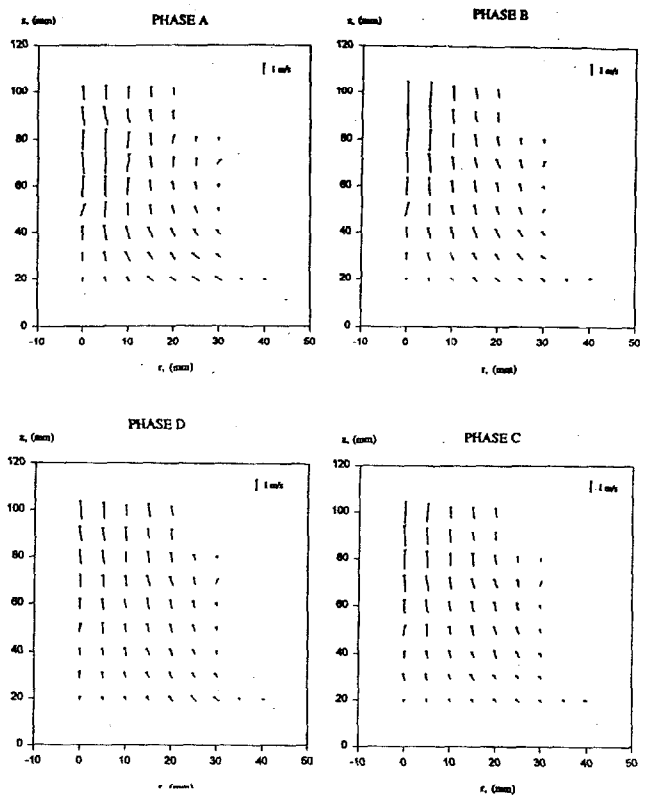

Figure 8 (right). Velocity distributions at four different phases during pulsation cycle for d = 10 cm. nozzle $Ri_1 = 50$.

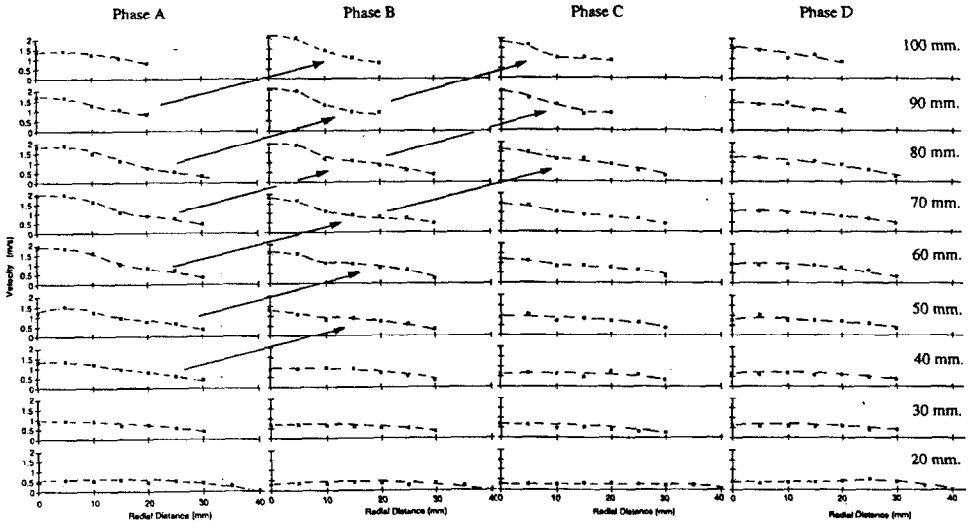

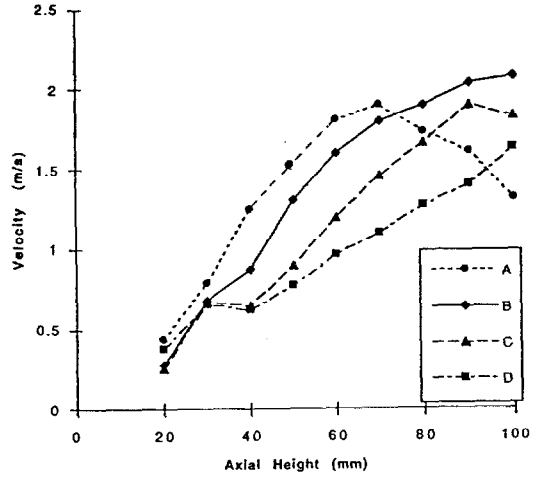

Figure 9.(top) Vertical component of velocity vector throughout the lower part of the plume in Figure 8.

Figure 10.(left) Plume centerline velocity profiles of the same plume depicted in Figures 8 and 9.

Discussion

Gunnar Heskestad: This is a very interesting field. Lot's of research still to do. For instance, in your helium experiments, it seems to me that it should be possible to correlate them without any scatter if we include viscosity and perhaps, density differences of the fluid being discharged.

Baki Cetegen: I agree with you. Those effects should be characterized by further experimentation. What we showed here is the first bit of it, if you will, to look at and include the difference which should be there in the correlation of frequency scaling. The viscosity effects should be looked at. They could introduce secondary effects, but this scaling seems, so far at least, to do well for the data we have.

Gunnar Heskestad: The second part of my question is when we correlating and scaling frequencies and diffusion flames, it seems to me that the flame height ought to be of some consequence for a given diameter.

Baki Cetegen: Yes, in fact, the paper done by Ed Zukoski and me had looked at the effects on the flame height fluctuations. If I understand your question correctly, yes, it has a consequence on the flame height fluctuations and that has been quantified to my knowledge by Ed's Symposium paper.

Edward Zukoski: I think what Gunnar was asking was if you increase the size of the fire, would the frequency change. And what we found was with the accuracy we were measuring, it did not. What did happen was the flapping with the low fuel flow was all the way down to the burner at the bottom. In contrast, when you had a high fuel flow, the flapping was up here. But the remarkable fact is, the frequency was within 10%.

Baki Cetegen: I would like to add that if you use our technique and if you increase the velocity at the source of the plume, you see a small change in the frequency and Anthony Hamins also pointed that out. However, the first-order effect which is the square root of the diameter, that's not affected as Ed said, within 10%. That appears to be constant. But if you look carefully, there is an effect on source velocity and that changes the frequency a little bit.

Henri Mitler: I think it's a pity that people can't leave well enough alone. There was a nice result of a square root and people continue to pick at this. Can you add some clarifying words, for example, between the square root result and the 0.4 result? Both of them are theoretically sensible, but it would be nice to try to get them harmonized.

Baki Cetegen: I think the issue is not leaving the problem alone, it's a different type of situation. In one case, you have local heat release in the flame. In this case, it's just a source buoyancy, so the problem is different. Now, with regard to resolving the 0.4 to 0.5, I'm assuming you are talking about flames. I don't have a good answer for that.